ACS APPLIED MATERIALS & INTERFACES

Forum Article

www.acsami.org

In Situ Infrared Ellipsometry for Protein Adsorption Studies on Ultrathin Smart Polymer Brushes in Aqueous Environment

Annika Kroning,[†,‡] Andreas Furchner,[†,‡] Dennis Aulich,[‡] Eva Bittrich,[§] Sebastian Rauch,[§] Petra Uhlmann,[§] Klaus-Jochen Eichhorn,[§] Michael Seeber,[⊥] Igor Luzinov,[⊥] S. Michael Kilbey II,[∥] Bradley S. Lokitz,[#] Sergiy Minko,[▽] and Karsten Hinrichs*[,‡]

[‡]Leibniz-Institut für Analytische Wissenschaften − ISAS − e. V., Schwarzschildstraße 8, 12489 Berlin, Germany

[§]Leibniz-Institut für Polymerforschung Dresden e. V., Hohe Straße 6, 01069 Dresden, Germany

[⊥]School of Materials Science and Engineering Clemson University, 161 Sirrine Hall, Clemson, South Carolina 29634-0971, United States

[∥]Departments of Chemistry and of Chemical Engineering, University of Tennessee, Knoxville, Tennessee 37996, United States

[#]Center for Nanophase Materials Sciences, Oak Ridge National Laboratory, Oak Ridge, Tennessee 37831, United States

[▽]Department of Chemistry, University of Georgia, Athens, Georgia 30602, United States

ABSTRACT: The protein-adsorbing and -repelling properties of various smart nanometer-thin polymer brushes containing poly(*N*-isopropylacrylamide) and poly(acrylic acid) with high potential for biosensing and biomedical applications are studied by in situ infrared-spectroscopic ellipsometry (IRSE). IRSE is a highly sensitive nondestructive technique that allows protein adsorption on polymer brushes to be investigated in an aqueous environment as external stimuli, such as temperature and pH, are varied. These changes are relevant to conditions for regulation of protein adsorption and desorption for biotechnology, biocatalysis, and bioanalytical applications. Here brushes are used as model surfaces for controlling protein adsorption of human serum albumin and human fibrinogen. The important finding of this work is that IRSE in the in situ experiments in protein solutions can distinguish between contributions of polymer brushes and proteins. The vibrational bands of the polymers provide insights into the hydration state of the brushes, whereas the protein-specific amide bands are related to changes of the protein secondary structure.

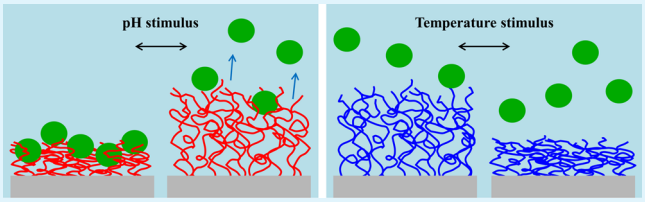

KEYWORDS: *polymer brushes, protein adsorption, solid−liquid interface, in situ infrared ellipsometry, stimuli-responsive, infrared spectroscopy*

1. INTRODUCTION

Polymer brushes are thin films of polymer molecules covalently attached to the substrate and unidirectionally stretched because of excluded volume interactions. Brushes modify surface properties, and by choosing a suitable polymer, the surface characteristics can be altered. Interfacial layers made from responsive polymers are especially relevant for biological or biosensing applications,[1,2] because external stimuli, such as temperature or pH, can switch the brushes between at least two states, thereby tuning the surface characteristics.[3−6]

Thermoresponsive polymers that have a swelling transition in the physiological temperature range have been of special interest for biological applications.[1,7−9] One example is poly(*N*-isopropylacrylamide) [PNIPAAm], which exhibits a lower critical solution temperature (LCST) behavior around 33 °C in water.[10] Brush layers of this polymer are very stable and can be switched reversibly between a swollen and a collapsed state.[11,12]

PNIPAAm brushes are known for their protein-repellent[1,13−16] as well as protein-adsorbing[17−19] characteristics, depending on the molecular weight and grafting density of the chains. For certain biomedical applications, it is essential that the surfaces do not adsorb proteins or other biomolecules,[20,21] whereas other applications demand the control of protein or cell adsorption and desorption.[19,21,22] Examples for the latter case are PNIPAAm-*co*-PGMA [poly(glycidyl methacrylate)] surfaces[8] or PNIPAAm brushes with low grafting density[19] for cell tissue engineering. To functionalize protein-repellent PNIPAAm layers for cell attachment, the polymer can also be modified with peptides.[23]

Examples for pH-responsive mixed polymer systems are poly(acrylic acid)/polystyrene [PAA/PS] brushes,[7] poly(2-vinylpyridine)/poly(acrylic acid) [P2VP/PAA] brushes,[24] P2VP/PNIPAAm brushes,[14,25] and PNIPAAm/PAA brushes.[26]

Special Issue: Forum on Polymeric Nanostructures: Recent Advances toward Applications

Received: October 31, 2014
Accepted: January 28, 2015
Published: February 10, 2015

DOI: 10.1021/am5075997
ACS Appl. Mater. Interfaces 2015, 7, 12430−12439

Table 1. Parameters of PNIPAAm and PGMA-*b*-PNIPAAm Brushes (Number-Average and Weight-Average Molecular Weights M_n and M_w, Polydispersity Index M_w/M_n, Grafting Density σ, Thicknesses in Dry and Wet State without Protein, and Protein Experiment Conditions) Used for IRSE and AFM in Situ Studies

						thickness (nm)			
polymer brush	M_n (g/mol)	M_w (g/mol)	M_w/M_n	in situ method	σ (nm^{-2})	dry state	swollen	collapsed	protein experiment
PGMA	17 500	29 800	1.70	IRSE	0.11	2.5			FIB, pH 7.4, 25–40 °C
PNIPAAm	132 000	169 000	1.28	IRSE	0.07	14.5	57.0 (25 °C)	17.0 (45 °C)	HSA, pH 6.7, 25–40 °C
PGMA-*b*-PNIPAAm (70.6% PNIPAAm)	PGMA: 11 500	PGMA: 13 500	1.28	IRSE	0.50	26.8			FIB, pH 7.4, 25–43 °C
	PNIPAAm: 24 200	PNIPAAm: 32 400		AFM	0.45	24.1	32.0 (23 °C)	30.9 (40 °C)	
PGMA-*b*-PNIPAAm (40.8% PNIPAAm)	PGMA: 36 600	PGMA: 43 900	1.13	IRSE	0.27	25.1			FIB, pH 7.4, 25–43 °C
	PNIPAAm: 28 900	PNIPAAm: 30 200		AFM	0.25	23.0	26.7 (25 °C)	27.2 (40 °C)	

The surface properties of PAA-containing systems are governed by the dissociation of carboxylic groups, which induces swelling of the brush with increasing pH because of increasing segment–segment repulsion and the osmotic pressure of counterions that enter the brush.[3,27−29] Those brushes allow for the controlled adsorption and desorption of proteins, tunable by pH changes of the solution.[7,30−32]

Understanding the adsorption properties of proteins on surfaces is a complex problem[33] that depends on the structure and shape of the protein and the geometry of the surface as well as on protein–surface interactions. Additionally, mixed switchable brushes may change the adsorption characteristics not only by a different chemical structure, composition, and geometry but also by mechanical and electrostatic repulsion.[7]

The requirement of a nondestructive characterization method for polymer brushes, applicable in aqueous solutions without labeling, restricts the choice of available analytic methods, especially when quantification and chemical specificity are needed at the same time. Methods of choice are vibrational spectroscopy (IR, Raman, sum frequency generation),[34,35] infrared and visible (VIS) ellipsometry,[3,7,12,14,24,26,35] atomic force microscopy (AFM),[36,37] fluorescence,[38] and neutron scattering.[15,39] With in situ visible and infrared ellipsometry, for instance, it is possible to study ultrathin brushes in liquid environments, such as different solvents, water, or other aqueous solutions. In a previous investigation,[7] we used in situ VIS ellipsometry and AFM force–distance measurements to measure, and consequently tune, the swelling behavior and the hydrophobic surface properties of mixed polymer brush surfaces for controlling protein adsorption on such surfaces.

Ellipsometry in the infrared spectral range allows direct access to the vibrational bands associated with the polymer functional groups of brushes and proteins. These bands provide a variety of information about surface structure and interactions. IR ellipsometry enables monitoring changes in the brushes that occur upon stimuli-dependent switching as well as upon adsorption of biomolecules down to the monolayer level. Additionally, one can obtain swollen thickness and water content of the brushes via optical simulations.[40]

In the present study, we focus on ultrathin brushes with dry layer thicknesses of less than 30 nm, for which the brush response to the stimulus occurs throughout the entire layer. In thicker brushes, the changing signal of the top layer would be overlapped by the less-changing signal of the underlying bulk layer.[15] Moreover, brush parameters like the grafting density are easily adjustable in the preparation of ultrathin brushes, which in the future might be favorable for tuning the protein-adsorbing properties.

We use in situ IR and VIS ellipsometry to study adsorption, structure, and interactions of human serum albumin (HSA) and fibrinogen (FIB) on various smart polymer films and brushes: on the one hand, a PNIPAAm brush in comparison to block copolymer PGMA-*b*-PNIPAAm brushes as examples for protein-repelling surfaces, and on the other hand, a PAA brush and an ultrathin PGMA film as examples for protein-adsorbing surfaces. HSA is chosen as a model protein for pH-dependent adsorption experiments on PAA brushes because of its pH stability, as will be shown later. For reasons of comparability with literature data, HSA is also used for adsorption studies on pure PNIPAAm brushes. Fibrinogen has a higher affinity to irreversibly adsorb to hydrophobic surfaces than HSA[41,42] and is therefore a good indicator for the influence of PGMA fractions on the PGMA-*b*-PNIPAAm copolymer brushes.

The focus of our study is the fingerprint region (1800–1300 cm^{-1}) where the most prominent bands for functional groups on the polymer chains and amide I and II bands of proteins are observed. The latter refer mainly to the C=O stretching and N–H bending mode of the peptide bond between the amino acids of the protein molecule. The amide bands are highly sensitive toward structural changes of the protein and provide sensitive information about interactions with the surface.

2. EXPERIMENTAL SECTION

2.1. Instrumental Set-ups. The principle of ellipsometry[43,44] is based on the change of polarization states of light upon reflection or transmission at an interface, where the incident linearly polarized light is converted into elliptically polarized light. The resulting polarization state is analyzed by using different polarizer settings to determine the amplitude ratio tan Ψ and the phase difference Δ between the complex reflection coefficients parallel (r_p) and perpendicular (r_s) to the plane of incidence

$$\tan \Psi \times e^{i\Delta} = \frac{r_p}{r_s} \quad (1)$$

Infrared spectroscopic ellipsometry was performed with a custom-built ellipsometer attached to a Bruker Vertex 70 spectrometer.[45] For the in situ measurements, a specially designed in situ cell[40,46] was used where the brush–solution interface is probed through an infrared-transparent silicon substrate. The cell is PID-temperature-controlled (PS01, OsTech GmbH i. G., Berlin, Germany) without overshoots and with a stability of ±0.05 °C.

DOI: 10.1021/am5075997
ACS Appl. Mater. Interfaces 2015, 7, 12430–12439

Table 2. Parameters of the Two PAA Brushes Used for IRSE and VIS-Ellipsometric in Situ Studies

						thickness (nm)		
polymer brush	M_n (g/mol)	M_w (g/mol)	M_w/M_n	in situ method	σ (nm^{-2})	dry state	pH 5.0	protein experiment
PAA	26 500	29 700	1.12	IRSE	0.22	6.9		HSA, pH 5.0–7.0, 25 °C
				VIS	0.15	4.7	39.7	

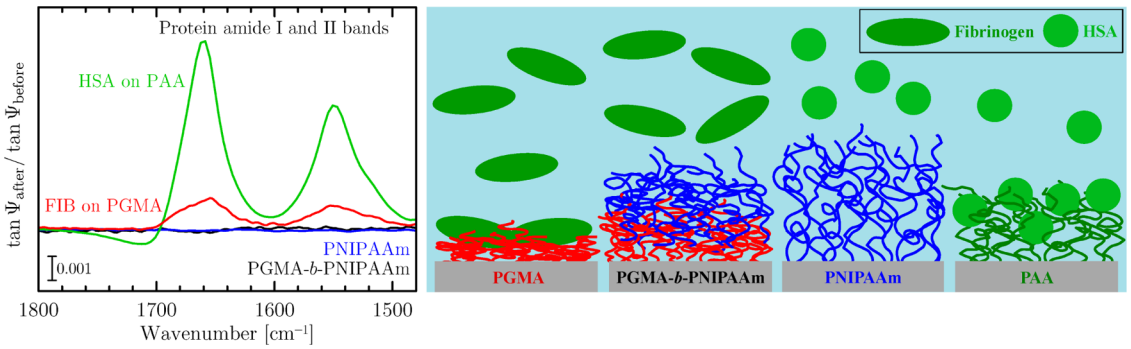

Figure 1. Right: Schematic overview of the polymer brushes/films and proteins studied in this work. Left: In situ tan Ψ spectra of different ultrathin polymer brushes/films after exposure to protein solutions, referenced to spectra of the initial film states in protein-free buffer. The PGMA-*b*-PNIPAAm copolymer brush contains 40.8% PNIPAAm.

Visible ellipsometry measurements were performed using an M-2000 diode-array rotating compensator ellipsometer (J. A. Woollam Co., Inc., Lincoln NE, USA) combined with a custom-made temperature-controlled in situ flow cell.[12]

AFM measurements were performed on a Bruker Dimension Icon in PeakForce quantitative nanomechanical property mapping mode.

2.2. Synthesis and Characterization of the Polymer Brush Films. Polymer brushes were prepared on silicon wafers (for VIS ellipsometry measurements and in situ AFM) and silicon wedges (1.5° wedge angle, for IR ellipsometry measurements) in two different ways via the "grafting-to" technique.[2,25] In the first approach, PNIPAAm and PAA brushes were synthesized in a two-step process.[12,25] A 2.5 nm thin layer of PGMA (M_n = 17 500 g/mol, M_w/M_n = 1.70, Polymer Source) was deposited by spin-coating a solution of 0.02 wt % PGMA in chloroform with subsequent annealing at 100 °C in a vacuum oven for 20 min to react the silanol groups of the substrate with a fraction of PGMA's epoxy groups. The resulting anchoring layer, which is self-cross-linked via ester bonds, is equipped with remaining epoxy groups for the following grafting step of PAA (M_n = 26 500 g/mol, M_w/M_n = 1.12, Polymer Source) or COOH-functionalized PNIPAAm chains (M_n = 132 000 g/mol, M_w/M_n = 1.28, Polymer Source). These were spin-coated from 1 wt % in ethanol and 1 wt % in tetrahydrofuran, respectively, and then annealed at 80 °C for 30 min in the case of PAA and at 150 °C for 19 h in the case of PNIPAAm.

In the second approach, brushes were made using PGMA-*b*-PNIPAAm block copolymers which were prepared via reversible addition–fragmentation chain transfer polymerization[47] from GMA and NIPAAm monomers. Their molecular weights and polydispersity indices were determined via gel permeation chromatography. The copolymers were dip-coated (Mayer Feintechnik D-3400, speed 240 mm/min) from 0.75 wt % polymer in MEK and annealed at 130 °C for 16 h. Details on the preparation process are described elsewhere.[47]

The brush parameters are summarized in Tables 1 and 2. The thicknesses of the dry brush layers were determined with VIS ellipsometry in ambient atmosphere (all brushes) and with AFM under nitrogen flow (PGMA-*b*-PNIPAAm brushes). The thicknesses in aqueous solution were determined with IRSE/VIS ellipsometry (pure PNIPAAm and PAA brushes) and AFM (PGMA-*b*-PNIPAAm brushes). To measure the thickness with AFM, the step edge was scanned after scratching away a part of the polymer layer with a needle. For each sample, the dry, swollen, and collapsed state were scanned on the same spot.

Grafting densities σ of the brushes were calculated according to

$$\sigma = N_A d\rho / M_n \quad (2)$$

with N_A being the Avogadro constant and d being the film thicknesses from ellipsometry. The polymer densities $\rho_{PNIPAAm}$ = 1.05 g/cm^3 and ρ_{PGMA} = 1.27 g/cm^3 (computed with Polymer Design Tools v. 1.1) as well as ρ_{PAA} = 1.40 g/cm^3 for PAA[48] were used for the pure brushes. Densities ρ of the PGMA-*b*-PNIPAAm copolymer brushes were calculated as the M_n-weighted average of the PGMA and PNIPAAm densities.

2.3. Protein Experiments. Buffer solutions with a concentration of 10 mM for the in situ ellipsometry experiments were either prepared from phosphate buffered saline (PBS) tablets (pH 7.4) purchased from Sigma-Aldrich, or from sodium phosphate monobasic dihydrate and sodium phosphate dibasic dihydrate at the desired pH. For the protein experiments, 0.25 mg/mL of human fibrinogen (Calbiochem) or defatted human serum albumin (Sigma-Aldrich) were dissolved in buffer solution.

It is known that fibrinogen adsorbs well on silicon surfaces.[41] Therefore, a control experiment was performed by adsorbing fibrinogen on a cleaned silicon wedge to obtain in situ tan Ψ spectra of a fibrinogen layer and to determine the position and shape of the corresponding amide bands. The adsorption on silicon was conducted in PBS solution at pH 7.4, first at 25 °C for 2 h, followed by an increase in temperature up to 45 °C, again keeping the temperature constant for 2 h, and then decreasing the temperature again to 25 °C for a third measurement, and a last measurement after a buffer rinse at 25 °C.

A second control experiment of fibrinogen adsorption on a 2.5 nm thin self-cross-linked PGMA layer was conducted under similar conditions. The sample was immersed in fibrinogen solution and measured at 25 °C for 2 h, followed by heating to 40 °C for 1 h, and at last a measurement after a buffer rinse at 25 °C.

Protein adsorption experiments on PNIPAAm and PGMA-*b*-PNIPAAm brushes were performed as follows: First, measurements of the brush in protein-free buffer solution were taken at different temperatures between 25 and 45 °C as a reference. Then, protein was added to the buffer solution and spectra were recorded at the same temperatures as the reference measurements, followed by a rinsing step in which the protein solution was replaced by a buffer solution with measurements made thereafter.

HSA adsorption and desorption on PAA brushes were measured with in situ IRSE under the following conditions: (1) Protein-free buffer at pH 5.0, (2) HSA solution at pH 5.0, (3) protein-free buffer at pH 5.4, 5.7, 6.0, 6.2, and 7.0. Before each pH change, ellipsometric

DOI: 10.1021/am5075997
ACS Appl. Mater. Interfaces 2015, 7, 12430–12439

measurements of the protein amide bands were repeated until an equilibrium of adsorption and desorption was reached. In situ VIS ellipsometry of the swelling of a PAA brush as well as HSA adsorption and desorption thereon were performed at pH 5, 6, and 7, again after waiting for equilibration of the brush−protein system after each pH change.

3. RESULTS AND DISCUSSION

To give an overview of the different adsorption properties of PNIPAAm, PGMA-*b*-PNIPAAm, PGMA, and PAA brushes, Figure 1 compares in situ tan Ψ spectra of the respective polymer film in protein solution after equilibration, referenced to protein-free buffer solution. Referenced in situ tan Ψ spectra are a measure of the change in optical contrast of the brush−solution interface. If proteins adsorb to the polymer, upward-pointing vibrational amide I and II bands associated with the protein structure will become visible. This is clearly the case for the PAA brush and the ultrathin PGMA film, showing their protein-adsorbing characteristics with respect to HSA and FIB, respectively. In contrast, no changes are observed in the tan Ψ spectra of PNIPAAm and PGMA-*b*-PNIPAAm brushes, thus demonstrating their protein-repellent surface properties. In the following sections, we discuss details of the protein-repelling and protein-adsorbing brushes.

3.1. Protein-Repelling Polymer Brushes Containing PNIPAAm. Both the template (PNIPAAm) and the adsorbing protein (fibrinogen) contain amide groups. Knowledge of the protein's amide bands is therefore necessary to distinguish the protein infrared signature from the brush signature. Results of fibrinogen adsorption on bare silicon are shown in Figure 2 (top), expressed by measured tan Ψ spectra of the silicon substrate in protein solution normalized to measured tan Ψ spectra of the same substrate in buffer solution at the corresponding temperatures. Fibrinogen adsorption is evidenced by the presence of strong amide I and II bands around 1650 and 1550 cm^{-1}, respectively. Subsequent spectra at 25, 45, and again 25 °C show a continuous thickness increase of the adsorbed layer over the course of 6 h. The amplitude ratio and shape of the amide I and II bands do not differ when adsorption takes place at 25 or 45 °C, the latter being below the temperature of the first denaturation step of the protein.[49,50] This means that the structure of adsorbed FIB protein does not change in the measured temperature range. A subsequent tan Ψ measurement of the adsorbed FIB layer in protein-free PBS at 25 °C shows no changes in the amide bands, indicating that the protein is strongly adsorbed on the silicon substrate. After the in situ experiment, the average protein layer thickness and refractive index in dry state were determined with ex situ VIS ellipsometry, resulting in d_{dry} = (20 ± 2) nm and n_∞ = 1.65. These values are consistent with the dimensions of fibrinogen[41] (~6 × 6 × 48 nm^3) and the optical properties of adsorbed fibrinogen as reported by Arwin.[51]

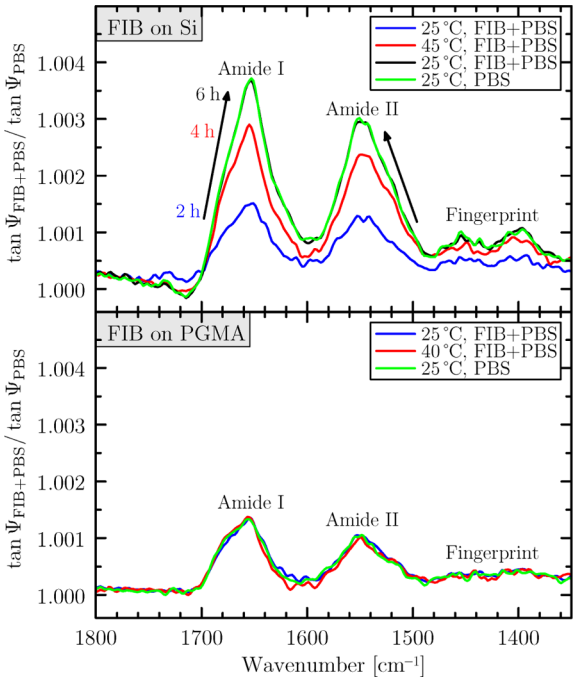

Figure 2. Top: In situ tan Ψ spectra of fibrinogen (FIB) adsorption on a silicon surface from a 0.25 mg/mL solution in PBS at pH 7.4 at 25 and 45 °C, referenced to protein-free buffer before the adsorption (tan Ψ_{PBS}). The blue, red, and black spectra are in chronological order with increasing band intensities. The green spectrum was measured in protein-free PBS after FIB adsorption. Bottom: Corresponding in situ tan Ψ spectra of fibrinogen adsorption on a 2.5 nm thin PGMA film.

To verify the protein-adsorbing surface properties of PGMA, we measured fibrinogen adsorption on a 2.5 nm ultrathin PGMA film. Maximum adsorption (i.e., maximum amide band amplitudes) occurred within the first 10 min of exposure of the film to protein solution. Compared to adsorption on silicon, no band changes were observed when raising the temperature to 40 °C. The amide I and II band shapes of the protein do not differ from those measured on silicon, implying that the structure of the adsorbed protein is similar in both cases. Nevertheless, the lower band intensities show that a much thinner protein layer is formed on PGMA, probably due to different film−protein interactions at the more hydrophobic PGMA surface. Note that the PGMA film is strongly self-cross-linked, which allows only for secondary protein adsorption[52] (on top of the film).

Infrared spectra are in general highly sensitive to amount and structure of the adsorbed protein layer. This is seen in ex situ tan Ψ measurements of the dried PGMA−FIB film after the protein experiment (top panel of Figure 3). The blue-shifted amide I and the red-shifted amide II band indicate the dehydration of the adsorbed protein layer, similar to collapsed PNIPAAm brushes, as will be discussed later. VIS ellipsometry on the dried PGMA−FIB layer resulted in a film thickness of d_{dry} = (7 ± 1) nm, indicating side-on adsorption of the rod-shaped fibrinogen molecules. In contrast to the thin PGMA film, no permanent fibrinogen adsorption (<0.5 nm) occurs on the PGMA-*b*-PNIPAAm copolymer brushes, as exemplarily demonstrated in Figure 3 (bottom) by ex situ tan Ψ spectra of the PNIPAAm-*b*-PGMA brush with 40.8% PNIPAAm content. The amide bands of PNIPAAm are not overlapped by fibrinogen amide bands. Furthermore, the brush structure was not modified by the presence of proteins in solution, as can be seen from the nonchanging PNIPAAm amide bands. Similar to the results reported by Lokitz et al.,[53] this indicates that although the layer contains more than 50% PGMA, its surface is dominated by the PNIPAAm blocks, resulting in a protein-repellent brush.

To understand the vibrational features of brush and protein in in situ IRSE spectra, the switching behavior of the brushes has to be analyzed first in the absence of protein. Figure 4 (left) compares in situ tan Ψ spectra of PGMA-*b*-PNIPAAm copolymer brushes with 70.6% and 40.8% PNIPAAm content

DOI: 10.1021/am5075997
ACS Appl. Mater. Interfaces 2015, 7, 12430−12439

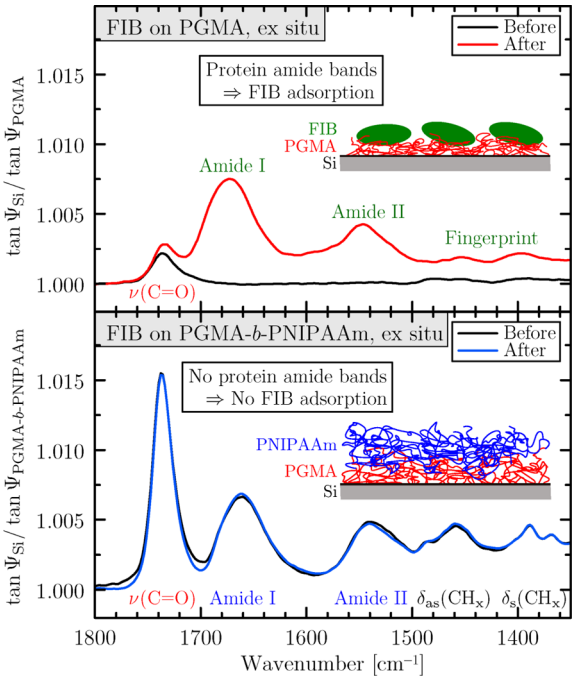

Figure 3. Top: Ex situ tan Ψ spectra (referenced to bare silicon substrate, tan Ψ_{Si}) of the 2.5 nm thin protein-adsorbing PGMA film measured in dry state before and after the fibrinogen adsorption experiment. Bottom: Corresponding ex situ tan Ψ spectra of the protein-repelling PNIPAAm-*b*-PGMA copolymer brush with 40.8% PNIPAAm.

(lower spectra) with those of a pure PNIPAAm brush (upper spectra). The blue and red lines refer to the swollen and collapsed state of the brushes, measured at 25 and 40 °C (43 °C), respectively. The temperature-dependent changes in the amide I and II vibrational bands are associated with the switching behavior of the brushes around their volume phase transition (LCST behavior). Similar to PNIPAAm chains in solution,[4] the amide I band in the swollen, strongly hydrated state contains at least two major components.[12] One is related to C═O groups fully hydrated by water molecules (~1625 cm^{-1}), and the other is due in part to C═O hydrogen-bond interactions with H−N of neighboring PNIPAAm amide groups (~1652 cm^{-1}). Above the LCST in the dehydrated state, the latter component dominates the amide I compositions, indicating the collapse of the brushes. Likewise, the amide II band consists of two components that are associated with water-hydrated N−H groups (~1558 cm^{-1}) and N−H groups interacting with other amide groups, the latter of which is shifted to lower wavenumbers. The amide I and II compositions in the pure PNIPAAm brush spectra in Figure 4 (left) differ notably from those of the PGMA-*b*-PNIPAAm copolymer brush with 70.6% PNIPAAm content. For the pure PNIPAAm brush in the swollen state, the 1625 cm^{-1} amide I and the 1558 cm^{-1} amide II components dominate. After the brush collapsed above the LCST, a pronounced switching in the band compositions is observed, i.e., the 1625 cm^{-1} component decreases in amplitude and the 1652 cm^{-1} component increases. The amide I band of the copolymer brush, however, is strongly governed by C═O···H−N interactions (~1652 cm^{-1}) in both the swollen and the collapsed states. Band changes of amide I are generally less pronounced than in the pure brush. Furthermore, the amide II band of the copolymer brush shows only a small redshift with increasing temperature, indicating less N−H groups interacting with surrounding water molecules. These band changes suggest that the PNIPAAm block in the copolymer undergoes a weaker transition with a smaller decrease in water content and C═O··· H_2O hydrogen bonding within the collapsed layer.

The LCST behavior (hydrogen bonding and swelling) is likely to depend on certain brush parameters, such as grafting density of the chains or the molecular weight of the PNIPAAm block.[13] Comparing the band compositions in the left panel of Figure 4 shows that amide I and II undergo much weaker band changes with decreasing PNIPAAm content. Almost no transition in amide I is found at 40.8% PNIPAAm content. At both low and high temperatures, the amide I band of this copolymer brush is dominated by stretching vibrations of fully hydrated C═O groups (~1625 cm^{-1}). Only a small part of the PNIPAAm segments switches to form C═O···H−N interactions (~1652 cm^{-1}), meaning that the copolymer brush does not collapse like a classical pure PNIPAAm brush. This

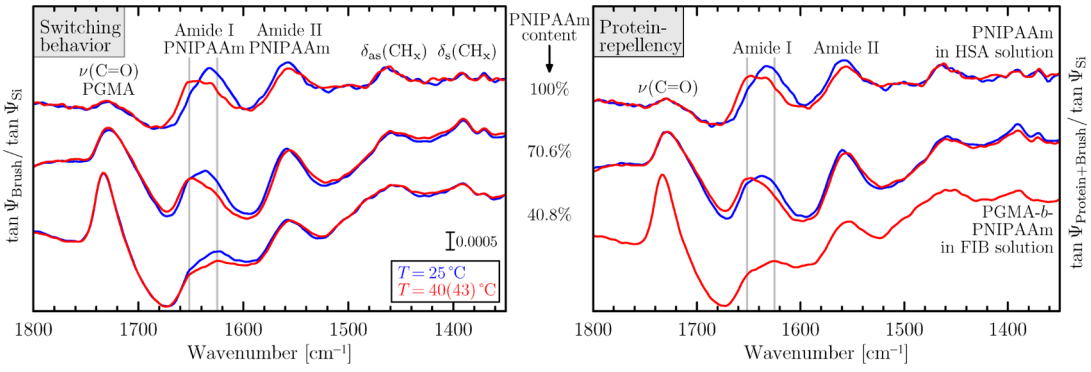

Figure 4. Left: Comparison of in situ tan Ψ spectra in protein-free solution of the pure PNIPAAm brush (100%) at 25 and 40 °C with those of PNIPAAm-*b*-PGMA copolymer brushes with 70.6 and 40.8% PNIPAAm content at 25 and 43 °C. The amide I/II bands of the copolymer brushes indicate a less pronounced switching behavior for brushes with decreasing PNIPAAm content. Note that the different interfaces (silicon/solution vs brush/solution) cause an overlap of amide I by a downward-pointing $\delta(H_2O)$ band, which shifts the measured band components of amide I (vertical gray lines) in dependence of thickness and water content of the brushes. Right: In situ tan Ψ spectra of a pure PNIPAAm brush in HSA solution at 25 and 40 °C compared with those of the PNIPAAm-*b*-PGMA copolymer brushes in fibrinogen solution at (25 °C and) 43 °C. Spectra are referenced to tan Ψ_{Si} of bare silicon substrate in protein-free buffer. Comparing the spectra to the switching signatures in protein-free solution (left), no differences are observed, that is, no protein adsorption takes place.

DOI: 10.1021/am5075997
ACS Appl. Mater. Interfaces 2015, 7, 12430−12439

nondeswelling behavior is also supported by in situ AFM measurements (see Table 1).

The differences in the switching behavior might be explained by interactions and steric hindrance of PNIPAAm with PGMA in the PGMA/PNIPAAm interpenetration layer. This layer results from cross-linking between different PGMA segments, which causes parts of the PNIPAAm blocks to emerge from within the PGMA layer, rather than from its surface.

Turning now to the in situ protein-adsorption IRSE studies on PNIPAAm-containing brushes, the right panel of Figure 4 shows similar in situ switching spectra of PGMA-*b*-PNIPAAm and PNIPAAm brushes as in Figure 4 (left), but this time measured with the brushes immersed in protein-containing buffer solutions. Comparison of the PGMA-*b*-PNIPAAm spectra with the corresponding spectra in the left panel shows that no protein adsorption takes place (surface concentration $\Gamma \ll 0.5$ mg/m^2), as is evidenced by the absence of vibrational bands attributable to fibrinogen. It is worth noting that even when the brushes are collapsed at elevated temperatures, no fibrinogen adsorption is observed, which suggests that the brush surfaces are dominated by the PNIPAAm blocks both in the swollen as well as in the collapsed states. These protein-repellent characteristics as well as the small swelling degree of the PGMA-*b*-PNIPAAm brushes in water (Table 1) indicate that only the top part of the brushes is hydrated in aqueous solution. This hydrated part sufficiently covers the underlying PGMA-rich part of the polymer layer, thus screening hydrophobic interactions between PGMA and fibrinogen. Similar findings of swollen brushes hiding their hydrophobic parts within the brush were obtained by Yu et al.[1] on PNIPAAm-*b*-PS brushes and Hoy et al.[7] on PEG/PAA-*b*-PS brushes. The same protein-repelling properties as for the PGMA-*b*-PNIPAAm brushes are found for the pure PNIPAAm brush in HSA solution. No HSA-related vibrational bands are observed.

The protein-repelling properties of the investigated PNIPAAm-containing brushes are in agreement with literature studies of protein-repelling[1,13−16,19] ($\Gamma < 0.5$ mg/m^2) and protein-adsorbing[17−19] ($\Gamma > 0.5$ mg/m^2) PNIPAAm surfaces. These suggest that adsorption rather occurs for end-grafted films with small molecular weight (film thicknesses smaller than 10 nm), for low grafting densities close to the transition/mushroom regime,[54] and above the LCST where water becomes a less good solvent for PNIPAAm. Yu et al.,[16] for example, showed a protein-repellent behavior with HSA adsorption levels $\Gamma < 0.2$ mg/m^2, both below and above the LCST for PNIPAAm layer thickness of 4−15 nm and a grafting density of $\sigma = 0.46$ nm^{-2}. Burkert et al.[14] measured PNIPAAm brushes with $\sigma = 0.06$−0.22 nm^{-2} and thicknesses of 5.1−15.7 nm. HSA adsorption was only nonzero ($\Gamma = 0.05$ mg/m^2) for the thinnest brush at 40 °C. Reversible protein adsorption was observed by Huber et al.[17] for ∼4 nm ultrathin PNIPAAm layers, presumably not in the brush regime. Xue et al.[19] studied adsorption of bovine serum albumin (BSA) in dependence of grafting density and found an almost constant low adsorption of about 0.2 mg/m^2 below the LCST, but increasing adsorption levels up to 0.9 mg/m^2 for a small grafting density of 0.01 nm^{-2} of a 5 nm ultrathin brush (M_n = 27 000 g/mol). For high grafting densities >0.10 nm^{-2}, BSA adsorption was smaller than 0.3 mg/m^2, even above the LCST.

The brushes investigated in the present study are thicker than 14 nm, exhibit grafting densities larger than 0.07 nm^{-2}, and/or have sufficiently long PNIPAAm chains (M_n = 132 000 g/mol for the pure PNIPAAm brush) in order for them to repel proteins both below and above the LCST. This is expected below the LCST where the brushes are in their hydrated, hydrophilic state. Above the LCST, the brushes are dehydrated and presumably constitute hydrophobic films. However, there is still a non-negligible number of C═O···H_2O interactions (1625 cm^{-1} amide I component in Figure 4) and a remaining average water content of several 10 vol %.[12,14,40,55,15,56] The observed protein-repelling surface properties, then, can be explained by the hydrophilic properties of the strongly hydrated topmost fraction of the brushes, which is supported by the neutron-reflectometry studies.[55,15,56] Systematic LCST studies with varying grafting density, molecular weight, and PNIPAAm content remain necessary to identify the transition between a generally protein-repelling brush and a surface with temperature-switchable repelling and adsorbing characteristics. This will allow one to design PGMA-*b*-PNIPAAm copolymer brushes for tunable protein-adsorption.

In summary, the investigated PNIPAAm and PGMA-*b*-PNIPAAm brushes constitute protein-repelling switchable surfaces. The high sensitivity of in situ IRSE allowed us to exclude adsorption effects and to attribute the observed band changes to structural changes within the brushes.

3.2. Protein-Adsorbing Poly(acrylic acid) Brushes.

Interpreting pH-dependent infrared spectra of PAA brushes with adsorbed HSA requires information about the stability of the protein structure in the measured pH range. Infrared transmission spectra of HSA solutions at pH 5 and 7, displayed in the top panel of Figure 5, show the $\delta(CH_x)$ fingerprint region as well as the amide I and II vibrational bands of HSA, the latter of which are highly sensitive toward changes of the protein secondary structure. The measured bands compare well with literature data[57] and indicate that HSA does not undergo structural changes with increasing pH. HSA can therefore be considered intact at both pH values. This knowledge is crucial for the following band assignments of the PAA−HSA system.

HSA adsorption at a PAA brush was monitored infrared-ellipsometrically using the characteristic amide I and II bands of the protein. The final protein-saturated brush state corresponds to the topmost brown spectrum in Figure 5 (middle). The absolute magnitude of HSA's amide bands indicates ternary protein adsorption,[52] that is, protein adsorption within the brush. This is supported by optical simulations and in situ VIS ellipsometry, as will be discussed later. Moreover, shapes and relative amplitudes of the HSA bands are in agreement with those obtained from HSA in solution (Figure 5, top). We therefore conclude that the protein structure remains unaltered upon adsorption.

Controlled protein desorption was then monitored during the stepwise increase of the buffer solution's pH from 5.0 to 7.0. Corresponding spectra are also shown in the middle panel of Figure 5. At first glance, the changing amplitude ratio between amide I and amide II is suggesting drastic alterations of the protein's secondary structure of remaining, i.e., still-adsorbed, HSA. However, the presence of protein within the brush as well as the increasing pH of the buffer solution both induce effects of PAA's carboxylic groups, responsible for the observed change of the amplitude ratio. The resulting infrared signatures are similar to those of a pure PAA brush pH-switched in buffer solution,[3] as is displayed in the bottom panel of Figure 5. Two upward-pointing bands, associated with stretching vibrations of COO^-, are overlapping the amide II and fingerprint bands of HSA. The peak position of amide I, however, is only slightly

DOI: 10.1021/am5075997
ACS Appl. Mater. Interfaces 2015, 7, 12430−12439

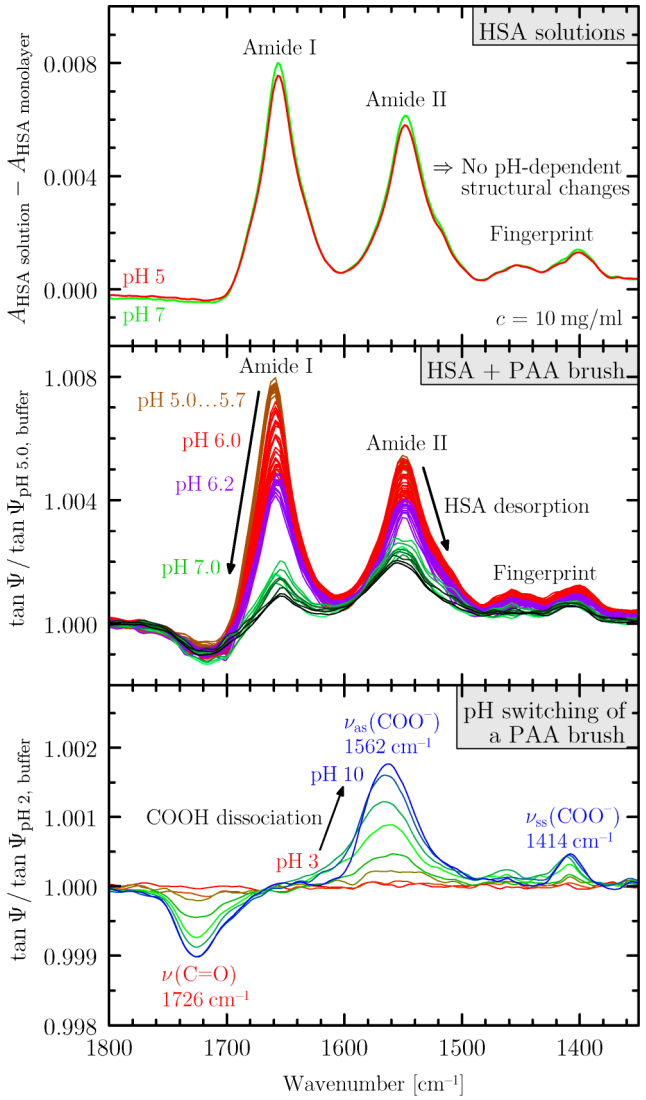

Figure 5. Top: Absorbances of HSA solutions with concentrations of c = (10.0 ± 0.2) mg/mL at pH 5 and 7 measured in transmission at 25 °C. Spectra are subtracted by absorbances of HSA monolayers in contact with protein-free buffer. Middle: Recorded tan Ψ spectra during HSA desorption from a PAA brush with increasing pH, referenced to the initial protein-free buffer solution at pH 5. Bottom: Switching behavior of a PAA brush between pH 2 and pH 10. Reprinted with permission from ref 3. Copyright 2010 American Chemical Society. All tan Ψ spectra are referenced to the initial spectrum at pH 2.

overlapped by the downward-pointing ν(COOH) band. Thus, in first-order approximation, amide I is a good quantitative indicator of the amount of adsorbed protein, rendering in situ IRSE a highly sensitive method for monitoring protein adsorption on such brushes.

The time-dependent amplitude of HSA's amide I band during the adsorption and desorption processes is plotted in Figure 6. Protein adsorption from the pH 5.0 solution reaches a maximum after about 120 min. After exchanging the solution for protein-free buffer at pH 5.4, the relative amplitude change of amide I is smaller than 2% compared to the last adsorption spectrum at pH 5.0. This suggests that adsorbed proteins stay attached to the brush and that only loosely bound proteins are removed. At pH 5.7—at the isoelectric point (IEP) of defatted HSA—the infrared signature still presents no notable changes. This is explained by the intrinsic pH value inside the brush, which generally differs from the one in solution.[3,27,58] The desorption process of HSA is initiated at pH 6.0. tan Ψ spectra recorded over a period of 68 min (red lines in the middle panel of Figure 5) show exponentially decreasing HSA band amplitudes toward a stable point at which desorption and readsorption are in equilibrium. The amide I peak diminishes to about 60% of its initial values. HSA seems to desorb due to its negative net charge above the IEP, resulting in electrostatic repulsion from the likewise negatively charged brush. Over the next 92 min, the pH value of the buffer was increased to 6.2 (purple lines) and finally to 7.0 (green to black lines). This leads to further desorption evidenced by a continuing decrease of the amide I amplitude, the absolute value of which diminishes to 12%. In the linear-amplitude approximation, this value is a good estimate of the relative amount of protein remaining adsorbed to or within the brush compared to the starting conditions at pH 5.4.

We confirmed the infrared-ellipsometric measurements with in situ VIS-ellipsometry measurements of HSA adsorption on a comparable PAA brush (see Table 2). Corresponding spectra provide complementary information via optical modeling, since the visible spectral range is free of absorption bands and is mainly governed by the Cauchy-like spectral behavior of PAA, buffer, and protein. Figure 7 displays the pH-dependent thickness of the combined PAA−HSA brush−protein layer, the percentage of buffer solution within that layer, as well as the absolute amount of adsorbed protein. The latter was derived using a modified de Feijter approach,[31,59] which assumes that the refractive index of a protein in solution is a linear function of the protein concentration. The approach is based on thickness, refractive index, and refractive index increment of the PAA−HSA layer[31] as well as the refractive index of the solution. All measurements were taken after equilibration of the sample. The shown data of the brush with adsorbed HSA correspond to the amide I amplitudes in Figure 6 measured at t = [112, 139, 252, 347] min.

At pH 5 without protein, the brush contains 89 vol % buffer and is already swollen by a factor of 8.5 compared to the dry state, in accordance with the partial dissociation of PAA's carboxylic groups.[3] After exchanging the buffer for HSA solution, the brush thickness increased from 39.7 to 43.8 nm, with Γ_{HSA} = 25.8 mg/m^2 adsorbed HSA, and decreased again to 42.1 nm after replacing the solution for protein-free buffer. This deswelling of the brush−protein layer confirms the previous observations of a slightly diminishing amide I band when exchanging the HSA solution for protein-free buffer. At pH 6, partial protein desorption takes place. Simultaneously, the brush begins to swell because of COOH dissociation, while binding additional buffer solution. At pH 7, most proteins desorb, with 14% remaining adsorbed to the brush compared to the pH 5 state. This value agrees with the amide I amplitude of 12% at the final desorption state at pH 7.0 compared to the initial state at pH 5.4 in the in situ infrared-ellipsometry measurements.

The results are in agreement with bovine-serum-albumin adsorption studies on planar PAA brushes.[30,31] De Vos et al.,[30] for instance, investigated the influence of polymer length, grafting density, and salt concentration on the pH-dependent adsorption behavior. They found adsorption maxima around pH 5.0−5.4 at a salt concentration of 10 mM. The amount of adsorbed BSA increased with both increasing polymer length and grafting density as well as with decreasing salt

DOI: 10.1021/am5075997
ACS Appl. Mater. Interfaces 2015, 7, 12430−12439

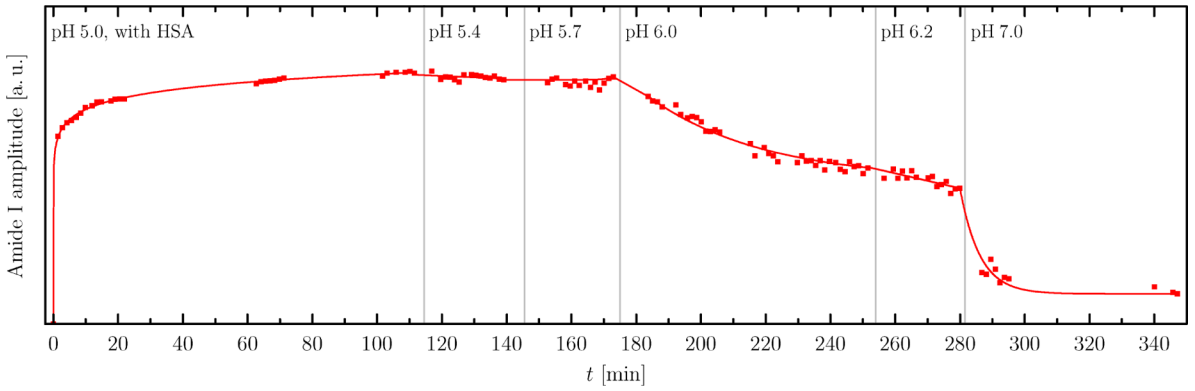

Figure 6. Time-dependent (85 s resolution) tan Ψ band amplitudes (|"Peak height" − 1.000|) of amide I in Figure 5 (middle) during HSA adsorption at pH 5.0, and controlled HSA desorption with increasing pH. To guide the eye, points during adsorption and desorption were connected by fitting "Ampl. ∝ $t^a/(t^a + b^a)$" with free parameters a and b, and with exponential-decay functions, respectively.

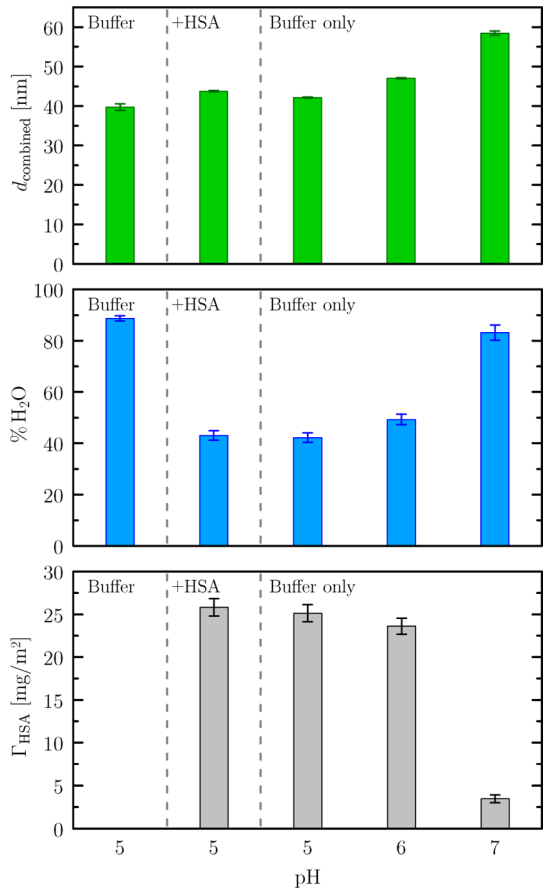

Figure 7. pH-dependent thickness $d_{combined}$ of the combined PAA–HSA brush–protein layer, % H_2O of buffer within the layer, as well as the absolute amount of ternary adsorbed protein Γ_{HSA}.

concentration. For PAA brushes with 270 monomer units and grafting densities between σ = 0.10–0.20 nm^{-2}, they have measured Γ_{BSA} = 16–25 mg/m^2 at pH 5, Γ_{BSA} = 13–20 mg/m^2 at pH 6, and $\Gamma_{BSA} \approx 2$ mg/m^2 at pH 7. These values compare well with data of the PAA brush with 368 monomer units and σ = 0.15 nm^{-2} presented in Figure 7.

Despite the lacking spectral contrast in the visible range, VIS ellipsometry is sensitive toward the various modes of protein adsorption,[52] that is, primary, secondary, and ternary adsorption. Simulations using the layer model "substrate/brush/protein/solution" (i.e., secondary adsorption) cannot reproduce the measured VIS ellipsometry data, whereas optical modeling with an effective brush–protein layer[31] can. This shows that the majority of proteins is indeed involved in ternary adsorption, which is consistent with the in situ IRSE amide band amplitudes and with experimental data by Rosenfeldt et al.[32] who have verified the penetration of bovine serum albumin into PAA brushes using small-angle X-ray scattering. VIS ellipsometry reaches its detection limit for small amounts of adsorbed protein with Γ_{HSA} < 0.1 mg/m^2.[12] Infrared ellipsometry as a complementary method in these cases provides a high enough spectral contrast with a sensitivity even to monolayer or submonolayer adsorption. Furthermore, additional information about stimuli-dependent brush and protein structure and chemistry as well as interactions is accessible.

4. CONCLUSIONS

We have demonstrated the potential of in situ spectroscopic ellipsometry at the solid–liquid interface for the detection of adsorbed proteins, their structural properties, and their interactions with stimuli-responsive smart polymer brushes. The high sensitivity of IRSE, meaning the presence or lack of protein-specific amide bands, allowed us to demonstrate the protein-repelling characteristics of temperature-responsive PNIPAAm and PGMA-*b*-PNIPAAm brushes, both in their swollen and collapsed states. pH-responsive PAA brushes, on the other hand, adsorb a substantial amount of human serum albumin at pH 5.0. Controlled protein desorption was then achieved by raising the pH to 7.0. Optical modeling of complementary VIS-ellipsometric spectra enabled the quantitative determination of swollen-brush thickness, buffer content, and amount of adsorbed protein, showing that almost 90% of the initially adsorbed protein molecules have desorbed. Additionally, the switching behavior of the brushes can be studied in the infrared spectral range by inspection of characteristic vibrational bands. Differences in the amide I and II bands of PNIPAAm are related to changing amide–amide and amide–water hydrogen-bond interactions. Similarly, the dissociation behavior of PAA brushes and the adsorption/desorption of HSA were monitored in situ by IRSE. Amide bands served as a quantitative indicator for the amount of adsorbed protein and allowed the conclusion that no structural changes of the proteins are occurring with increasing pH. This renders IRSE a suitable method for study of complex

DOI: 10.1021/am5075997
ACS Appl. Mater. Interfaces 2015, 7, 12430–12439

interactions in changeable environment of biointerfaces that involve functional polymers and protein molecules.

AUTHOR INFORMATION

Corresponding Author

*E-mail: karsten.hinrichs@isas.de.

Author Contributions

†A.K. and A.F. contributed equally to this work.

Notes

The authors declare no competing financial interest.

ACKNOWLEDGMENTS

The authors thank Manfred Stamm for support and interesting discussions over many years of collaboration in various research projects. They thank Ilona Engler for technical assistance in FT-IR spectroscopy. This work was supported by the *Deutsche Forschungsgemeinschaft* (Grant DFG Hi 793/4-1, Ei 317/4-1 and Sta 324/28-1) and the *National Science Foundation* (Grant DMR-1107786) within the Materials World Network. The block copolymers were synthesized at the Center for Nanophase Materials Sciences, which is a DOE Office of Science User Facility. S.M.K. acknowledges support from the National Science Foundation (Award 1133300).

REFERENCES

(1) Yu, Q.; Zhang, Y.; Chen, H.; Zhou, F.; Wu, Z.; Huang, H.; Brash, J. L. Protein Adsorption and Cell Adhesion/Detachment Behavior on Dual-Responsive Silicon Surfaces Modified with Poly(*N*-isopropylacrylamide)-*block*-polystyrene Copolymer. *Langmuir* **2010**, *26*, 8582−8588.

(2) Islam, M. R.; Ahiabu, A.; Li, X.; Serpe, M. J. Poly(*N*-isopropylacrylamide) Microgel-Based Optical Devices for Sensing and Biosensing. *Sensors* **2014**, *14*, 8984−8995.

(3) Aulich, D.; Hoy, O.; Luzinov, I.; Brücher, M.; Hergenröder, R.; Bittrich, E.; Eichhorn, K.-J.; Uhlmann, P.; Stamm, M.; Esser, N.; Hinrichs, K. In Situ Studies on the Switching Behavior of Ultrathin Poly(acrylic acid) Polyelectrolyte Brushes in Different Aqueous Environments. *Langmuir* **2010**, *26*, 12926−12932.

(4) Maeda, Y.; Higuchi, T.; Ikeda, I. Change in Hydration State During the Coil−Globule Transition of Aqueous Solutions of Poly(*N*-isopropylacrylamide) as Evidenced by FTIR Spectroscopy. *Langmuir* **2000**, *16*, 7503−7509.

(5) Pengxiang, J.; Yongkuan, G.; Shengqin, W.; Jiang, Z. Advantage of Fluorescence Correlation Spectroscopy for the Study of Polyelectrolytes. *Chin. J. Chem.* **2012**, *30*, 2237−2240.

(6) Zhou, J.; Wang, G.; Hu, J.; Lu, X.; Li, J. Temperature, Ionic Strength and pH Induced Electrochemical Switching of Smart Polymer Interfaces. *Chem. Commun.* **2006**, *46*, 4820−4822.

(7) Hoy, O.; Zdyrko, B.; Lupitskyy, R.; Sheparovych, R.; Aulich, D.; Wang, J.; Bittrich, E.; Eichhorn, K.-J.; Uhlmann, P.; Hinrichs, K.; Müller, M.; Stamm, M.; Minko, S.; Luzinov, I. Synthetic Hydrophilic Materials with Tunable Strength and a Range of Hydrophobic Interactions. *Adv. Funct. Mater.* **2010**, *20*, 2240−2247.

(8) Joseph, N.; Prasad, T.; Raj, V.; Anil Kumar, P. R.; Sreenivasan, K.; Kumary, T. V. A Cytocompatible Poly(*N*-isopropylacrylamide-*co*-glycidylmethacrylate) Coated Surface as New Substrate for Corneal Tissue Engineering. *J. Bioact. Compat. Polym.* **2010**, *25*, 58−74.

(9) Madathil, B. K.; Kumar, P. R. A. A.; Kumary, T. V. *N*-Isopropylacrylamide-*co*-glycidylmethacrylate as a Thermoresponsive Substrate for Corneal Endothelial Cell Sheet Engineering. *BioMed. Res. Int.* **2014**, Article ID 450672.

(10) Wang, X.; Qiu, X.; Wu, C. Comparison of the Coil-to-Globule and the Globule-to-Coil Transition of a Single Poly(*N*-isopropylacrylamide) Homopolymer Chain in Water. *Macromolecules* **1998**, *31*, 2972−2976.

(11) Takei, Y. G.; Aoki, T.; Sanui, K.; Ogata, N.; Sakurai, Y.; Okano, T. Dynamic Contact Angle Measurement of Temperature-Responsive Surface Properties for Poly(*N*-isopropylacrylamide) Grafted Surfaces. *Macromolecules* **1994**, *27*, 6163−6166.

(12) Bittrich, E.; Burkert, S.; Müller, M.; Eichhorn, K.-J.; Stamm, M.; Uhlmann, P. Temperature-Sensitive Swelling of Poly(*N*-isopropylacrylamide) Brushes with Low Molecular Weight and Grafting Density. *Langmuir* **2012**, *28*, 3439−3448.

(13) Xue, C.; Yonet-Tanyeri, N.; Brouette, N.; Sferrazza, M.; Braun, P. V.; Leckband, D. E. Protein Adsorption on Poly(*N*-isopropylacrylamide) Brushes: Dependence on Grafting Density and Chain Collapse. *Langmuir* **2011**, *27*, 8810−8818.

(14) Burkert, S.; Bittrich, E.; Kuntzsch, M.; Müller, M.; Eichhorn, K.-J.; Bellmann, C.; Uhlmann, P.; Stamm, M. Protein Resistance of PNIPAAm Brushes: Application to Switchable Protein Adsorption. *Langmuir* **2010**, *26*, 1786−1795.

(15) Brouette, N.; Xue, C.; Haertlein, M.; Moulin, M.; Fragneto, G.; Leckband, D. E.; Halperin, A.; Sferrazza, M. Protein Adsorption Properties of OEG Monolayers and Dense PNIPAAm Brushes Probed by Neutron Reflectivity. *Eur. Phys. J.: Spec. Top.* **2012**, *213*, 343−353.

(16) Yu, Q.; Zhang, Y.; Chen, H.; Wu, Z.; Huang, H.; Cheng, C. Protein Adsorption on Poly(*N*-isopropylacrylamide)-Modified Silicon Surfaces: Effects of Grafted Layer Thickness and Protein Size. *Colloids Surf., B* **2010**, *76*, 468−474.

(17) Huber, D. L.; Manginell, R. P.; Samara, M. A.; Kim, B.-I.; Bunker, B. C. Programmed Adsorption and Release of Proteins in a Microfluidic Device. *Science* **2003**, *301*, 352−354.

(18) Cheng, X.; Canavan, H. E.; Graham, D. J.; Castner, D. G.; Ratner, B. D. Temperature Dependent Activity and Structure of Adsorbed Proteins on Plasma Polymerized *N*-isopropyl acrylamide. *Biointerphases* **2006**, *1*, 61−72.

(19) Xue, C.; Choi, B.-C.; Choi, S.; Braun, P. V.; Leckband, D. E. Protein Adsorption Modes Determine Reversible Cell Attachment on Poly(*N*-isopropyl acrylamide) Brushes. *Adv. Funct. Mater.* **2012**, *22*, 2394−2401.

(20) Vroman, L. Methods of Investigating Protein Interactions on Artificial and Natural Surfaces. *Ann. N.Y. Acad. Sci.* **1987**, *516*, 300−305.

(21) Ratner, B. D.; Bryant, S. J. Biomaterials: Where We Have Been and Where We Are Going. *Annu. Rev. Biomed. Eng.* **2004**, *6*, 41−75.

(22) Yang, W.; Tang, Z.; Luan, Y.; Liu, W.; Li, D.; Chen, H. Thermoresponsive Copolymer Decorated Surface Enables Controlling the Adsorption of a Target Protein in Plasma. *ACS Appl. Mater. Interfaces* **2014**, *6*, 10146−10152.

(23) Halperin, A.; Kröger, M. Thermoresponsive Cell Culture Substrates Based on PNIPAm Brushes Functionalized with Adhesion Peptides: Theoretical Considerations of Mechanism and Design. *Langmuir* **2012**, *28*, 16623−16637.

(24) Uhlmann, P.; Houbenov, N.; Brenner, N.; Grundke, K.; Burkert, S.; Stamm, M. In-Situ Investigation of the Adsorption of Globular Model Proteins on Stimuli-Responsive Binary Polyelectrolyte Brushes. *Langmuir* **2007**, *23*, 57−64.

(25) Bittrich, E.; Burkert, S.; Eichhorn, K.-J.; Stamm, M.; Uhlmann, P. In *Proteins and Interfaces III State of the Art*; Horbett, T., Brash, J. L., Norde, W., Eds.; ACS Symposium Series; American Chemical Society: Washington, D.C., 2012; Vol. *1120*, Chapter 8, pp 179−193.

(26) Bittrich, E.; Kuntzsch, M.; Eichhorn, K.-J.; Uhlmann, P. Complex pH- and Temperature-Sensitive Swelling Behavior of Mixed Polymer Brushes. *J. Polym. Sci., Part B: Polym. Phys.* **2010**, *48*, 1606−1615.

(27) Dong, R.; Lindau, M.; Ober, C. K. Dissociation Behavior of Weak Polyelectrolyte Brushes on a Planar Surface. *Langmuir* **2009**, *25*, 4774−4779.

(28) Wu, T.; Gong, P.; Szleifer, I.; Vlček, P.; Šubr, V.; Genzer, J. Behavior of Surface-Anchored Poly(acrylic acid) Brushes with Grafting Density Gradients on Solid Substrates: 1. Experiment. *Macromolecules* **2007**, *40*, 8756−8764.

DOI: 10.1021/am5075997
ACS Appl. Mater. Interfaces 2015, 7, 12430−12439

(29) Toomey, R.; Tirrell, M. Functional Polymer Brushes in Aqueous Media from Self-Assembled and Surface-Initiated Polymers. *Annu. Rev. Phys. Chem.* **2008**, *59*, 493−517.
(30) De Vos, W. M.; Biesheuvel, M.; de Keizer, A.; Kleijn, J. M.; Cohen Stuart, M. A. Adsorption of the Protein Bovine Serum Albumin in a Planar Poly(acrylic acid) Brush Layer as Measured by Optical Reflectometry. *Langmuir* **2008**, *24*, 6575−6584.
(31) Bittrich, E.; Rodenhausen, K. B.; Eichhorn, K.-J.; Hofmann, T.; Schubert, M.; Stamm, M.; Uhlmann, P. Protein Adsorption on and Swelling of Polyelectrolyte Brushes: A Simultaneous Ellipsometry-Quartz Crystal Microbalance Study. *Biointerphases* **2010**, *5*, 159−167.
(32) Rosenfeldt, S.; Wittemann, A.; Ballauff, M.; Breininger, E.; Bolze, J.; Dingenouts, N. Interaction of Proteins with Spherical Polyelectrolyte Brushes in Solution as Studied by Small-Angle X-ray Scattering. *Phys. Rev. E* **2004**, *70*, 061403.
(33) Minko, S. Responsive Polymer Brushes. *J. Macromol. Sci., Polym. Rev.* **2006**, *46*, 397−420.
(34) Friedbacher, G.; Bubert, H., Eds. *Surface and Thin Film Analysis: A Compendium of Principles, Instrumentation, and Applications*; Wiley: Weinheim, Germany, 2011.
(35) Hinrichs, K.; Eichhorn, K.-J., Eds. *Ellipsometry of Functional Organic Surfaces and Films*; Springer: Heidelberg, Germany, 2014.
(36) García, R.; Pérez, R. Dynamic Atomic Force Microscopy Methods. *Surf. Sci. Rep.* **2002**, *47*, 197−301.
(37) Roiter, Y.; Minko, S. Adsorption of Polyelectrolyte versus Surface Charge: In Situ Single-Molecule Atomic Force Microscopy Experiments on Similarly, Oppositely, and Heterogeneously Charged Surfaces. *J. Phys. Chem. B* **2007**, *111*, 8597−8604.
(38) Sapsford, K. E.; Ligler, F. S. Real-time Analysis of Protein Adsorption to a Variety of Thin Films. *Biosens. Bioelectron.* **2004**, *19*, 1045−1055.
(39) Reinhardt, M.; Dzubiella, J.; Trapp, M.; Gutfreund, P.; Kreuzer, M.; Gröschel, A. H.; Müller, A. H. E.; Ballauff, M.; Steitz, R. Fine-Tuning the Structure of Stimuli-Responsive Polymer Films by Hydrostatic Pressure and Temperature. *Macromolecules* **2013**, *46*, 6541−6547.
(40) Furchner, A.; Bittrich, E.; Uhlmann, P.; Eichhorn, K.-J.; Hinrichs, K. In-Situ Characterization of the Temperature-Sensitive Swelling Behavior of Poly(*N*-isopropylacrylamide) Brushes by Infrared and Visible Ellipsometry. *Thin Solid Films* **2013**, *541*, 41−45.
(41) Tunc, S.; Maitz, M. F.; Steiner, G.; Vázquez, L.; Pham, M. T.; Salzer, R. In Situ Conformational Analysis of Fibrinogen Adsorbed on Si Surfaces. *Colloids Surf., B* **2005**, *42*, 219−225.
(42) Vörös, J. The Density and Refractive Index of Adsorbing Protein Layers. *Biophys. J.* **2004**, *87*, 553−561.
(43) Tompkins, H. G.; Irene, E. A., Eds. *Handbook of Ellipsometry*; Springer: Heidelberg, Germany, 2005.
(44) Röseler, A.; Korte, E.-H. In *Handbook of Vibrational Spectroscopy, Vol. 2*; Chalmers, J. M.; Griffiths, P. R., Eds.; John Wiley & Sons: Chichester, U.K., 2002; Chapter 2.8, pp 1065−1090.
(45) Korte, E.-H.; Hinrichs, K.; Röseler, A. Spectroscopic Infrared Ellipsometry to Determine the Structure of Layered Samples. *Spectrochim. Acta, Part B* **2002**, *57*, 1625−1634.
(46) Mikhaylova, Y.; Ionov, L.; Rappich, J.; Gensch, M.; Esser, N.; Minko, S.; Eichhorn, K.-J.; Stamm, M.; Hinrichs, K. In Situ Infrared Ellipsometric Study of Stimuli-Responsive Mixed Polyelectrolyte Brushes. *Anal. Chem.* **2007**, *79*, 7676−7682.
(47) Seeber, M. Synthesis and Characterization of Thermally Responsive Polymer Layers. *Ph.D. Thesis*, Clemson University, Clemson, SC, Paper 1138, 2013; http://tigerprints.clemson.edu/all_dissertations/1138.
(48) Ichinose, I.; Kawakami, T.; Kunitake, T. Alternate Molecular Layers of Metal Oxides and Hydroxyl Polymers Prepared by the Surface Sol-Gel Process. *Adv. Funct. Mater.* **1998**, *10*, 535−539.
(49) Marx, G.; Mou, X.; Hotovely-Salomon, A.; Levdansky, L.; Gaberman, E.; Belenky, D.; Gorodetsky, R. Heat Denaturation of Fibrinogen to Develop a Biomedical Matrix. *J. Biomed. Mater. Res. Part B* **2007**, *84B*, 49−57.
(50) Chen, Y.; Mao, H.; Zhang, X.; Gong, Y.; Zhao, N. Thermal Conformational Changes of Bovine Fibrinogen by Differential Scanning Calorimetry and Circular Dichroism. *Int. J. Biol. Macromol.* **1999**, *26*, 129−134.
(51) Arwin, H. Application of Ellipsometry Techniques to Biological Materials. *Thin Solid Films* **2011**, *519*, 2589−2592.
(52) Currie, E. P. K.; Norde, W.; Cohen Stuart, M. A. Tethered Polymer Chains: Surface Chemistry and their Impact on Colloidal and Surface Properties. *Adv. Colloid Interface Sci.* **2003**, *100−102*, 205−265.
(53) Lokitz, B. S.; Wei, J.; Hinestrosa, J. P.; Ivanov, I.; Browning, J. F.; Ankner, J. F.; Kilbey, S. M., II; Messman, J. M. Manipulating Interfaces through Surface Confinement of Poly(glycidyl methacrylate)-block-poly(vinyldimethylazlactone), a Dually Reactive Block Copolymer. *Macromolecules* **2012**, *45*, 6438−6449.
(54) Brittain, W. J.; Minko, S. A Structural Definition of Polymer Brushes. *J. Polym. Sci. Part A* **2007**, *45*, 3505−3512.
(55) Yim, H.; Kent, M. S.; Satija, S.; Mendez, S.; Balamurugan, S. S.; Balamurugan, S.; Lopez, G. P. Evidence for Vertical Phase Separation in Densely Grafted, High-Molecular-Weight Poly(*N*-isopropylacrylamide) Brushes in Water. *Phys. Rev. E* **2005**, *72*, 051801.
(56) Elliot, L. C. C.; Jing, B.; Akgun, B.; Zhu, Y.; Bohn, P. W.; Fullerton-Shirey, S. K. Loading and Distribution of a Model Small Molecule Drug in Poly(*N*-isopropylacrylamide) Brushes: a Neutron Reflectometry and AFM Study. *Langmuir* **2013**, *29*, 3259−3268.
(57) Barbucci, R.; Magnani, A. Conformation of Human Plasma Proteins at Polymer Surfaces: The Effectiveness of Surface Heparinization. *Biomaterials* **1994**, *15*, 955−962.
(58) Gong, P.; Wu, T.; Genzer, J.; Szleifer, I. Behavior of Surface-Anchored Poly(acrylic acid) Brushes with Grafting Density Gradients on Solid Substrates: 2. Theory. *Macromolecules* **2007**, *40*, 8765−8773.
(59) De Feijter, J. A.; Benjamins, J.; Veer, F. A. Ellipsometry as a Tool to Study the Adsorption Behavior of Synthetic and Biopolymers at the Air−Water Interface. *Biopolymers* **1978**, *17*, 1759−1772.

DOI: 10.1021/am5075997
ACS Appl. Mater. Interfaces 2015, 7, 12430−12439